Neuron
Article

Postsynaptic TrkC and Presynaptic PTPσ Function as a Bidirectional Excitatory Synaptic Organizing Complex

Hideto Takahashi,[1,2] Pamela Arstikaitis,[1,2] Tuhina Prasad,[1,2] Thomas E. Bartlett,[1,3] Yu Tian Wang,[1,3] Timothy H. Murphy,[1,2] and Ann Marie Craig[1,2,*]
[1]Brain Research Centre
[2]Department of Psychiatry
[3]Department of Medicine
University of British Columbia, Vancouver, British Columbia V6T 2B5, Canada
*Correspondence: amcraig@interchange.ubc.ca
DOI 10.1016/j.neuron.2010.12.024

SUMMARY

Neurotrophin receptor tyrosine kinases (Trks) have well-defined trophic roles in nervous system development through kinase activation by neurotrophins. Yet Trks have typical cell-adhesion domains and express noncatalytic isoforms, suggesting additional functions. Here we discovered noncatalytic TrkC in an unbiased hippocampal neuron-fibroblast coculture screen for proteins that trigger differentiation of neurotransmitter release sites in axons. All TrkC isoforms, but not TrkA or TrkB, function directly in excitatory glutamatergic synaptic adhesion by neurotrophin-independent high-affinity trans binding to axonal protein tyrosine phosphatase receptor PTPσ. PTPσ triggers and TrkC mediates clustering of postsynaptic molecules in dendrites, indicating bidirectional synaptic organizing functions. Effects of a TrkC-neutralizing antibody that blocks TrkC-PTPσ interaction and TrkC knockdown in culture and in vivo reveal essential roles of TrkC-PTPσ in glutamatergic synapse formation. Thus, postsynaptic TrkC trans interaction with presynaptic PTPσ generates bidirectional adhesion and recruitment essential for excitatory synapse development and positions these signaling molecules at the center of synaptic pathways.

INTRODUCTION

High-affinity neurotrophin receptors TrkA, TrkB, and TrkC are receptor tyrosine kinases that mediate the trophic effects of soluble target-derived neurotrophins via intracellular signaling cascades (Barbacid, 1994; Huang and Reichardt, 2003). Neurotrophin-induced Trk dimerization and activation via trans phosphorylation promote precursor proliferation and neuronal survival and differentiation. Previous studies show functional roles of neurotrophin and kinase-mediated activities of Trks in gene transcription (Segal and Greenberg, 1996), axonal and dendritic growth and remodeling (McAllister, 2001), and synapse maturation and plasticity (Poo, 2001). Structurally, in addition to the membrane-proximal neurotrophin-binding immunoglobulin-like domain (Ig2), all Trks contain an additional extracellular Ig domain (Ig1) and leucine-rich repeats flanked by cysteine clusters (LRRCC) (Huang and Reichardt, 2003; Urfer et al., 1995). These domains, typical of cell-adhesion molecules, are of unknown function in Trks. Furthermore, a significant fraction of TrkB and TrkC are broadly expressed in brain as noncatalytic isoforms, lacking tyrosine kinase domains (Barbacid, 1994; Valenzuela et al., 1993). The function of these noncatalytic Trk isoforms is not well understood, but is probably important, considering, for example, the more severe phenotype of TrkC null mice compared with mice lacking only the kinase-active isoforms of TrkC (Klein et al., 1994; Tessarollo et al., 1997). The fraction of noncatalytic relative to kinase-active Trk isoforms increases during the second and third postnatal weeks (Valenzuela et al., 1993), the peak period of synaptogenesis.

Synaptogenesis requires clustering of synaptic vesicles and the neurotransmitter release machinery in axons precisely apposed to chemically matched neurotransmitter receptors and associated scaffolding and signaling proteins in dendrites (Dalva et al., 2007; Shen and Scheiffele, 2010; Siddiqui and Craig, 2010). Two key steps include axon-dendrite physical contact mediated by cell-adhesion molecules and local recruitment of presynaptic and postsynaptic components mediated by synapse organizing or "synaptogenic" proteins. Many protein families contribute to synaptic differentiation, but few defined synaptic adhesion molecule complexes have bidirectional synaptogenic function. Neuroligin-neurexin (Graf et al., 2004; Scheiffele et al., 2000), LRRTM-neurexin (de Wit et al., 2009; Ko et al., 2009; Linhoff et al., 2009; Siddiqui et al., 2010) netrin G ligand 3 (NGL-3)-LAR (Woo et al., 2009) and EphB-ephrinB (Dalva et al., 2007) transsynaptic complexes mediate adhesion between dendrites and axons and trigger local pre- and postsynaptic differentiation. The in vivo importance of these proteins for synapse development is supported by knockout mouse and human disease studies. For example, neuroligin-1,2,3 triple knockout is perinatally lethal due to defects in synaptic transmission (Varoqueaux et al., 2006) and neuroligin-1 or −2 individual knockout mice exhibit selective defects in excitatory or inhibitory synapses, respectively

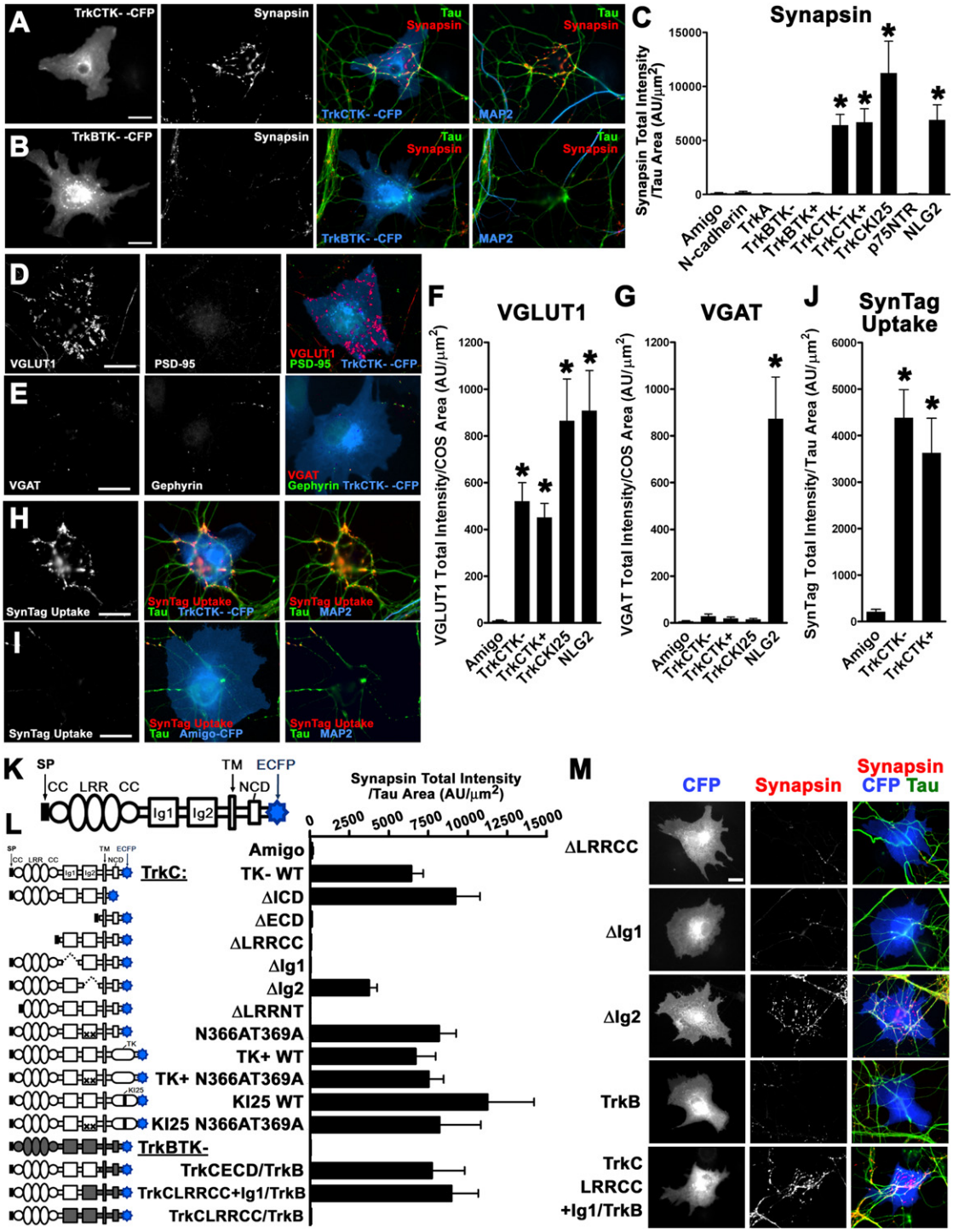

Figure 1. TrkC Expressed in COS Cells Induces Functional Excitatory Presynaptic Differentiation through its LRR and First Ig Domain

(A) COS cells expressing TrkCTK- induce synapsin clustering along contacting axons (labeled with dephosphorylated tau) lacking association with dendrites (labeled with MAP2).

(B) COS cells expressing TrkBTK- do not induce synapsin clustering along contacting axons.

(C) Quantification of the total integrated intensity of synapsin staining associated with COS cells expressing the indicated CFP fusion proteins and not associated with MAP2 divided by the tau-positive axon-contact area. ANOVA, $p < 0.0001$, $n \geq 20$ cells each; *$p < 0.01$ compared with Amigo by post hoc Dunnett's multiple comparison test.

(Chubykin et al., 2007). Copy number, promoter, and protein-truncating and missense variants in neuroligins, neurexins, and LRRTMs are linked to autism, schizophrenia, and mental retardation, emphasizing the importance of these genes for brain development and cognitive function (Francks et al., 2007; Jamain et al., 2003; Kim et al., 2008; Sudhof, 2008).

Recently, given the molecular and functional diversity of synapses, we have been working on globally identifying the full set of potent synaptogenic adhesion molecules by using an unbiased functional expression screen (Linhoff et al., 2009). We screened >10^5 clones of a custom postnatal brain full-length cDNA expression library in pools in a neuron-fibroblast coculture assay to identify factors able to trigger presynaptic differentiation in contacting hippocampal axons. From this screen, we reisolated neuroligin and NGL-3 and first identified LRRTMs as synaptogenic. Here, we report the isolation of neurotrophin receptor TrkC noncatalytic form as a synaptogenic adhesion molecule that triggers excitatory presynaptic differentiation. All TrkC isoforms, but not TrkA or TrkB, are synaptogenic via neurotrophin-independent binding to the axonal tyrosine phosphatase receptor PTPσ. Extensive induction, localization, and function-blocking experiments in vitro and in vivo support the conclusion that transsynaptic interaction between dendritic TrkC and axonal PTPσ generates bidirectional noncatalytic signaling essential for excitatory pre- and postsynaptic differentiation in neural network development.

RESULTS

An Unbiased Expression Screen Identifies Noncatalytic TrkC as Synaptogenic

Here, we continued the unbiased expression screen for mammalian synaptogenic proteins that trigger presynaptic differentiation when presented on COS cells to axons of cocultured hippocampal neurons (Linhoff et al., 2009). We subdivided PB270, one positive cDNA pool that contained about 250 clones, to identify the single clone responsible for its synaptogenic activity (Figures S1A and S1B, available online). Both positive single clones isolated, PDB 270-46-2-3H and PDB 270-46-17-9M, encode neurotrophin receptor tyrosine kinase TrkC, noncatalytic form (GenBank accession number: BC078844). This TrkC isoform, here called TrkCTK- (also known as TrkCic158, TrkCNC2, and TrkCT1), is the most abundant of four noncatalytic TrkC isoforms that through alternative splicing lack tyrosine kinase domains and have alternative shorter intracellular domains (Barbacid, 1994; Valenzuela et al., 1993).

TrkC Induces Differentiation of Functional Excitatory Presynaptic Terminals

We first tested whether all neurotrophin receptors induce presynaptic differentiation. We performed the coculture assay by using COS cells expressing each neurotrophin receptor tagged intracellularly with ECFP and quantified clustering of the presynaptic component synapsin in contacting axons. Only TrkC, but not TrkA, noncatalytic TrkB (TrkBTK-, also known as TrkB.T1), catalytic TrkB (TrkBTK+), or p75NTR low-affinity receptor, induced synapsin clustering in hippocampal axons (Figures 1A–1C). Surface protein expression of TrkA, TrkB, or p75NTR on COS cells was similar to or higher than that of TrkC (Figures S1C–S1H), suggesting that the lack of synaptogenic activity is not due to insufficient surface expression. TrkC catalytic forms (TrkCTK+ and TrkCKI25) as well as TrkCTK- all promoted synapsin clustering as efficiently as positive-control neuroligin-2 (NLG2), the most potent of the neuroligins (Figures 1A–1C).

Unlike neuroligins and NGL-3, which induce both excitatory and inhibitory presynaptic differentiation (Chih et al., 2005; Woo et al., 2009), all isoforms of TrkC induced only clustering of excitatory presynaptic marker VGLUT1, but not of inhibitory presynaptic marker VGAT in coculture (Figures 1D–1G). These results suggest not only that TrkC may function specifically at excitatory synapses but also that the presynaptic receptor of TrkC might be different from neurexins and LAR, the main presynaptic receptors for neuroligins and NGL-3, respectively (Sudhof, 2008; Woo et al., 2009). TrkCTK- or TrkCTK+ also induced uptake of antibodies against the lumenal domain of synaptotagmin I (SynTag), which is accessible on the neuron surface only during active recycling of synaptic vesicles (Figures 1H–1J). Together, these data indicate that TrkC induces the differentiation of functional excitatory presynaptic terminals.

The Synaptogenic Domain of TrkC Is Distinct from the Neurotrophin-Binding Site

TrkC binds to neurotrophin NT-3, but not to NGF or BDNF (Barbacid, 1994; Huang and Reichardt, 2003); Ig2 of TrkC is necessary and sufficient for NT-3 binding (Urfer et al., 1995). To determine the domains responsible for TrkC synaptogenic

(D) COS cells expressing TrkCTK- induce glutamatergic excitatory presynaptic marker VGLUT1 clustering in contacting axons. Absence of associated PSD-95 family proteins was used to exclude interneuronal synapses.
(E) COS cells expressing TrkCTK- do not induce GABAergic inhibitory presynaptic marker VGAT clustering in contacting axons.
(F and G) Quantification of the total integrated intensity of VGLUT1 (F) or VGAT (G) staining associated with COS cells expressing the indicated CFP fusion proteins. ANOVA, $p < 0.0001$, $n \geq 20$ cells each; *$p < 0.01$ compared with Amigo by Dunnett's multiple comparison test.
(H and I) COS cells expressing TrkCTK- (H) but not Amigo (I) induce functional presynaptic differentiation assessed by incubating with antibodies to synaptotagmin I (SynTag) luminal domain.
(J) Quantification of the total integrated intensity of uptaken SynTag luminal-domain antibody divided by the axon-contact area. ANOVA, $p < 0.0001$, $n \geq 20$ cells each; *$p < 0.01$ compared with Amigo by Dunnett's multiple comparison test.
(K) Structure of TrkCTK- -CFP. TrkCTK- has leucine-rich repeats (LRR) flanked by cysteine clusters (CC) and two immunoglobulin-like domains (Ig1 and Ig2) in the extracellular region, transmembrane domain (TM), and a noncatalytic domain (NCD) in the intracellular region.
(L) Quantification of the total integrated intensity of synapsin staining on tau-positive axons contacting COS cells expressing the indicated TrkC deletion and TrkB/TrkC swap mutants. ANOVA, $p < 0.0001$, $n \geq 20$ cells each.
(M) Representative synapsin images of the indicated TrkC deletion and TrkB/TrkC swap mutants in coculture assay. Scale bars: 20 μm. All error bars are SEM. See also Figure S1.

activity, we tested several TrkC deletion mutants by scoring synapsin clustering in the coculture assay. The TrkC extracellular domain (ECD) was necessary and sufficient for synaptogenic activity; the intracellular domain (ICD) was not required (Figure 1L). TrkC mutants lacking LRRCC, Ig1, or LRRNT, the initial part of LRRCC, did not have synaptogenic activity (Figures 1L and 1M). Lack of synaptogenic activity was not due to insufficient surface expression of these mutants (Figures S1C–S1H). The mutant lacking Ig2, the NT-3-binding domain, still had synaptogenic activity. We also tested TrkC containing point mutations that abolish NT-3 binding (N366AT369A) (Urfer et al., 1998). All noncatalytic and catalytic TrkC with NT-3-binding dead mutations still have synaptogenic activity (Figure 1L). These data indicate that NT-3 binding is not required and that both LRRCC and Ig1 are required for synaptogenic activity of TrkC.

To test whether TrkC LRRCC plus Ig1 is sufficient for synaptogenic activity, we used chimeras between TrkCTK- and the non-synaptogenic TrkBTK-. The ECD of TrkC, or just LRRCC plus IgG1 of TrkC, but not LRRCC alone, conferred synaptogenic activity on the TrkB chimera (Figures 1L and 1M). Thus, both the LRRCC and Ig1 of TrkC are necessary and sufficient for synaptogenic activity.

The TrkC Synaptogenic Domain Binds the Tyrosine Phosphatase Receptor PTPσ

TrkC in COS cells triggers presynaptic differentiation presumably through trans interaction with a presynaptic receptor on contacting axons. To identify the presynaptic receptor, we screened a range of candidate proteins, including neurexins, expressed in COS cells in a binding assay, by using soluble purified TrkC ectodomain fused to human immunoglobulin Fc region (TrkC-Fc) (Figure S2A). Only one candidate bound TrkC-Fc, protein tyrosine phosphatase receptor PTPσ.

PTPσ belongs to the type IIa subfamily of receptor tyrosine phosphatases, comprised of PTPσ, PTPδ, and LAR (Johnson and Van Vactor, 2003). Recent studies have shown that NGL-3 binds to PTPσ, PTPδ, and LAR via their first two fibronectin III-like domains (FNIII) (Kwon et al., 2010). In our binding assay, soluble TrkC-Fc proteins bound only to PTPσ, not to PTPδ or LAR, nor to N-cadherin or neurexin-1β (Figures 2A and 2B). Application of increasing amounts of TrkC-Fc to PTPσ-expressing COS cells revealed saturable binding (Figure 2C). According to Scatchard analysis, the apparent dissociation constant (Kd) value is 9.3 ± 1.2 nM, within the typical nanomolar range for biologically significant ligand-receptor interactions. TrkC still bound to PTPσ in nominally calcium-free buffer containing 10 mM EGTA (Figure 2D), suggesting Ca^{2+}-independent interaction. The PTPσ ectodomain is composed of three Ig-like domains followed by either four or eight FNIII domains, depending on splice variant. TrkC-Fc did not bind to a PTPσ mutant lacking all three Ig domains, but bound to a mutant lacking all FNIII domains (Figure 2E), indicating that the Ig domains of PTPσ are responsible for TrkC binding. Alternative splicing also occurs within the Ig region, inserting short sequences meA and/or meB (Pulido et al., 1995). TrkC-Fc bound to all isoforms of PTPσ, although differences in intensity of bound TrkC-Fc suggest a possible modulatory effect of meB (Figure 2E).

If axonal PTPσ mediates the synaptogenic activity of TrkC, PTPσ should bind to the synaptogenic region of TrkC, LRRCC plus Ig1 (Figure 1L). We tested this idea by using a soluble PTPσ ectodomain Fc fusion. PTPσ-Fc bound to COS cells expressing TrkCTK- wild-type, ΔIg2, and N366AT369A, but not to those expressing TrkCTK- ΔLRRCC, ΔIg1, or ΔLRRNT (Figures 2F and 2G). PTPσ-Fc also bound to the TrkB/C chimera TrkCLRRCC+Ig1/TrkBTK- but not to TrkCLRRCC/TrkBTK- or TrkB wild-type (Figures 2F and 2G). Taken together, these data indicate that the PTPσ-binding domain of TrkC is LRRCC and Ig1, supporting the idea that PTPσ is the presynaptic receptor through which TrkC triggers presynaptic differentiation.

We also tested whether TrkC or PTPσ might interact in a homophilic manner (Figure S2). However, in our cell-binding assay, PTPσ-Fc did not bind to PTPσ itself, PTPδ, or LAR. In addition, the TrkC ectodomain with NT-3-binding dead mutations fused to Fc (TrkCN366AT369A-Fc) bound to PTPσ but did not bind to either TrkC itself or to any other neurotrophin receptors.

TrkC and PTPσ Localize to Glutamatergic Synapses

We next investigated subcellular localization of TrkC and PTPσ in cultured hippocampal neurons. TrkC immunoreactivity with an antibody that detects all isoforms was present in a punctate pattern on dendrites of hippocampal neurons at DIV 15 (Figure 3A). TrkC puncta colocalized well with clusters of the excitatory postsynaptic scaffold PSD-95 apposed to VGLUT1 but not with the inhibitory postsynaptic scaffold gephyrin (Figures 3A and 3B). We tested specifically whether TrkCTK- and/or TrkCTK+ localize to excitatory synapses in hippocampal neurons by low-level expression of extracellularly YFP-tagged forms. Both YFP-TrkCTK- and YFP-TrkCTK+ accumulated at excitatory synaptic sites marked by PSD-95 clusters apposed to VGLUT1 clusters (Figures 3C and 3D). The presence of synaptic YFP-TrkC clusters in dendrites but not axons of transfected neurons indicated postsynaptic and not presynaptic accumulation. Immunofluorescence analysis also revealed TrkC immunoreactivity in a punctate pattern in neuropil of adult mouse brain. Moreover, TrkC puncta were apposed to VGLUT1 puncta but not to gephyrin puncta, as shown here for hippocampal CA1 region (Figures 3G–3I). These data indicate that TrkC localizes to excitatory synapses in vitro and in vivo.

PTPσ immunoreactivity was also present in a punctate pattern decorating the dendrites of cultured hippocampal neurons at DIV 15 and these puncta overlapped with VGLUT1 (Figure 3E). PTPσ puncta overlapping VGLUT1 were also observed on axons not contacting dendrites, suggesting an axonal localization (Figure 3E, arrowheads). PTPσ puncta were not colocalized with VGAT clusters (Figure 3F). Furthermore, PTPσ puncta were apposed to PSD-95 puncta in brain, as shown here for hippocampal CA1 region (Figure 3J). Thus, endogenous PTPσ is also localized to excitatory synaptic sites in vitro and in vivo.

Overexpression of TrkC in Neurons Promotes Excitatory Presynaptic Differentiation

Next, we tested the effects of TrkC overexpression (DIV9–10 → DIV14–15) in cultured hippocampal neurons. Overexpression of HA-TrkCTK- significantly enhanced synapsin clustering along

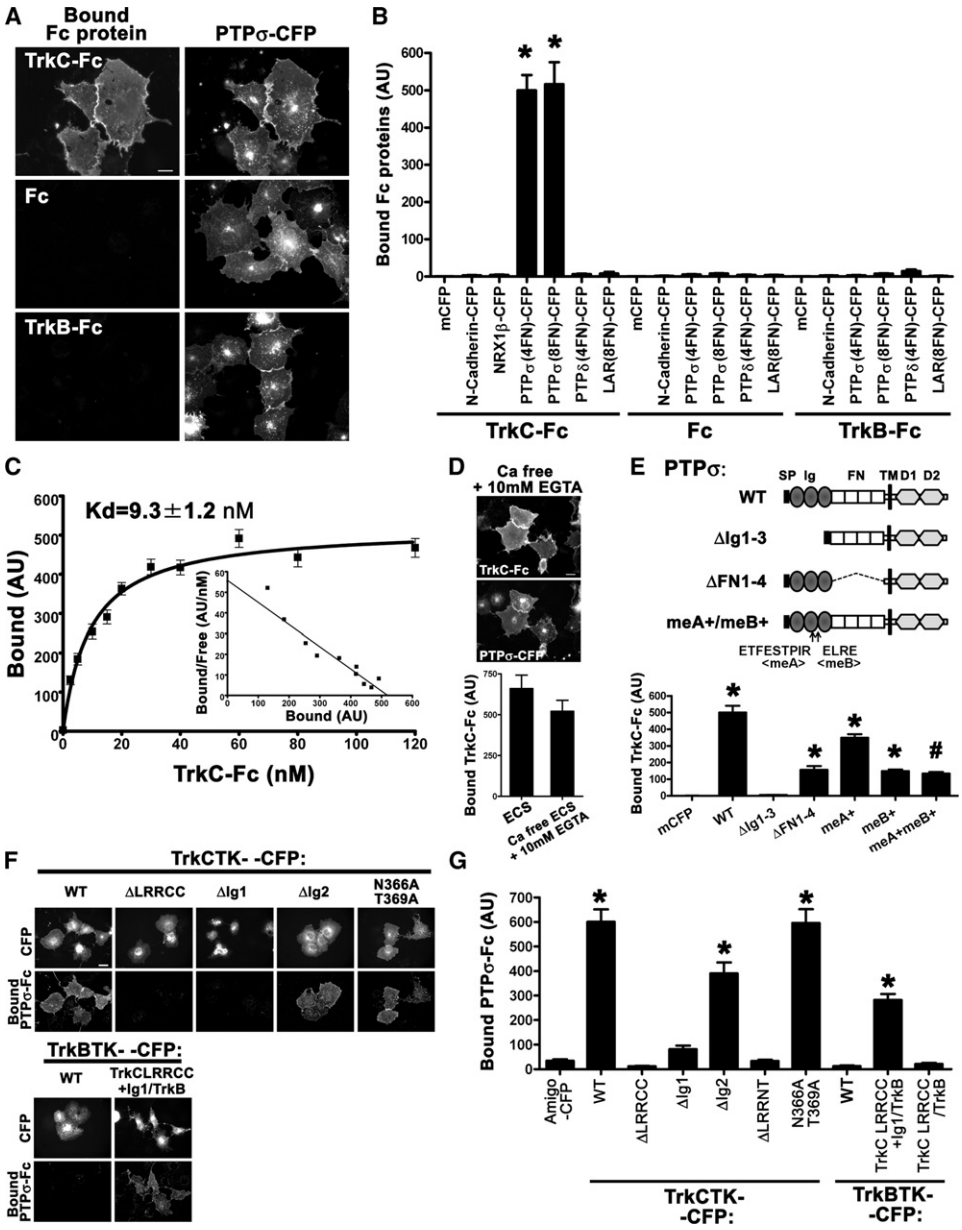

Figure 2. TrkC Binds with High Affinity to Tyrosine Phosphatase Receptor PTPσ

(A) We tested for binding of several candidates expressed in COS cells to TrkC-Fc. PTPσ-CFP specifically bound TrkC-Fc but not control Fc or TrkB-Fc.

(B) Quantification of Fc proteins bound to COS cells expressing the indicated constructs. TrkC-Fc bound PTPσ isoforms with four or eight fibronectin III-like domains (FN) but not PTPδ, LAR, neurexin1β (NRX1β), N-cadherin, or membrane-associated CFP (mCFP). ANOVA, $p < 0.0001$ for TrkC-Fc, $n \geq 20$ cells each; *$p < 0.01$ compared with mCFP by Dunnett's multiple comparison test.

(C) By Scatchard analysis, affinity of binding of TrkC-Fc to PTPσ-CFP was estimated at 9.3 nM ($n > 30$ cells each).

(D) Binding of TrkC-Fc to PTPσ-CFP did not require extracellular calcium. $p > 0.1$, Student's t test, $n > 40$ cells each.

(E) Domain analysis of PTPσ showed that the three Ig domains mediate binding to TrkC and alternative splicing within these regions may modulate binding affinity. ANOVA, $p < 0.0001$, $n > 20$ cells each; *$p < 0.01$ and #$p < 0.05$ compared with mCFP by Dunnett's multiple comparison test.

(F and G) PTPσ-Fc also bound to COS cells expressing TrkC-CFP. Domain analysis of TrkC showed that the LRR and first Ig domain mediate binding to PTPσ. ANOVA, $p < 0.0001$, $n > 20$ cells each; *$p < 0.01$ compared with Amigo by Dunnett's multiple comparison test. Scale bars: 20 μm. All error bars are SEM. See also Figure S2.

dendrites compared to neurons expressing only ECFP or neighboring nontransfected neurons (Figure S3). Overexpression of HA-TrkCTK+ resulted in an abnormal morphology of neurons with retracted or beaded dendrites and also enhanced synapsin clustering along these dendrites. Overexpression of HA-TrkCTK- or HA-TrkCTK+ enhanced clustering of VGLUT1 but not of VGAT

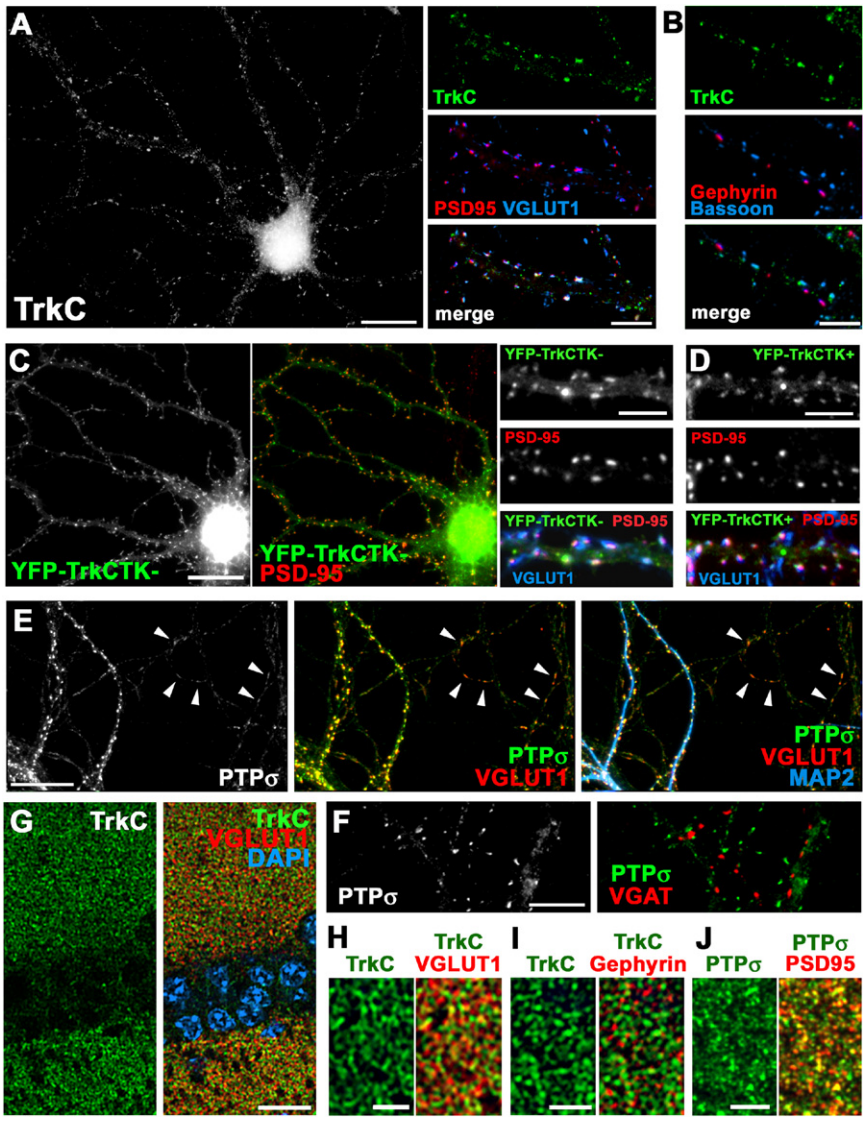

Figure 3. TrkC and PTPσ Localize to Glutamate Synapses

(A and B) Immunolocalization of TrkC in cultured hippocampal neurons shows coclustering at excitatory synapses colocalizing with PSD-95 and apposed to VGLUT1 (A) but no association with inhibitory synapses labeled with gephyrin (B).

(C and D) Recombinant YFP-TrkC noncatalytic (TK-) (C) or catalytic (TK+) (D) forms expressed at low level in cultured hippocampal neurons cluster in dendrites with PSD-95 apposed to VGLUT1.

(E and F) Immunolocalization of PTPσ in cultured hippocampal neurons shows coclustering at excitatory synapses labeled with VGLUT1 (E) but no association with inhibitory synapses labeled with VGAT (F). Small PTPσ puncta overlapping with VGLUT1 are also localized on axons not contacting dendrites (arrowheads).

(G–I) Immunolocalization of TrkC in mouse brain also shows TrkC clustering at excitatory synapses, as shown here, with apposition to VGLUT1 (G, H) but not gephyrin (I) in hippocampal CA1; enlarged region is from stratum radiatum.

(J) Immunolocalization of PTPσ in mouse brain also shows PTPσ clustering at excitatory synapses, as shown here, with apposition to PSD-95 in hippocampal CA1 stratum radiatum. Scale bars: 20 μm in A left panel, C left panel, E, F and G; 5 μm in the other panels. See also Figure S3.

along the dendrites (Figure S3), consistent with the results of coculture experiments. Thus, TrkC expressed in neurons exerts synaptogenic activity for excitatory presynaptic differentiation.

TrkC Beads Cluster Axonal PTPσ and Excitatory Presynaptic Proteins; PTPσ Beads Cluster Dendritic TrkC and Excitatory Postsynaptic Proteins

To assess whether any proteins from neurons or COS cells might be needed to cooperate with TrkC in promoting presynaptic differentiation, we investigated the synaptogenic activity of inert micron-sized beads coated with TrkC-Fc. Beads coated with TrkC-Fc, but not control Fc or TrkB-Fc, induced clustering of synapsin, the active-zone marker bassoon, and VGLUT, but not VGAT at contact sites with hippocampal axons (Figures S4A–S4F). Thus, the TrkC ectodomain is sufficient for induction of excitatory presynaptic differentiation. Furthermore, TrkC-Fc-coated beads that contact axons induced clustering of endogenous PTPσ with synapsin (Figures 4A–4C). Thus, PTPσ is expressed in axons, the TrkC ectodomain can bind to endogenous axonal PTPσ via trans interaction, and the TrkC ectodomain induces presynaptic differentiation associated with clustering of PTPσ.

To test whether PTPσ mediates TrkC-induced presynaptic differentiation, we investigated synapsin clustering around TrkC-Fc-coated beads that contacted axons expressing either HA-PTPσ or HA-PTPσ lacking the intracellular domain (HA-PTPσΔICD). TrkC-Fc-coated beads induced HA-PTPσ clustering accompanied by synapsin clustering on axons (Figures 4D and 4E). TrkC-induced synapsin clustering associated with HA-PTPσ was equivalent to TrkC-induced synapsin clustering on neighboring nontransfected axons (Figure 4E), suggesting that HA-PTPσ is comparable in activity to the endogenous presynaptic receptor of TrkC. In contrast, TrkC-Fc-coated beads that induced HA-PTPσΔICD clustering on axons did not induce simultaneous clustering of synapsin (Figures 4D and 4E). Presumably, HA-PTPσΔICD effectively competed with endogenous PTPσ for TrkC binding and blocked transmembrane signaling from TrkC to axonal intracellular targets for presynaptic differentiation. Taken together, these data suggest that PTPσ is an axonal receptor for TrkC that triggers presynaptic differentiation.

Next, we tested whether PTPσ ectodomain triggers excitatory postsynaptic differentiation associated with dendritic accumulation of TrkC. PTPσ-Fc-coated beads that contacted dendrites

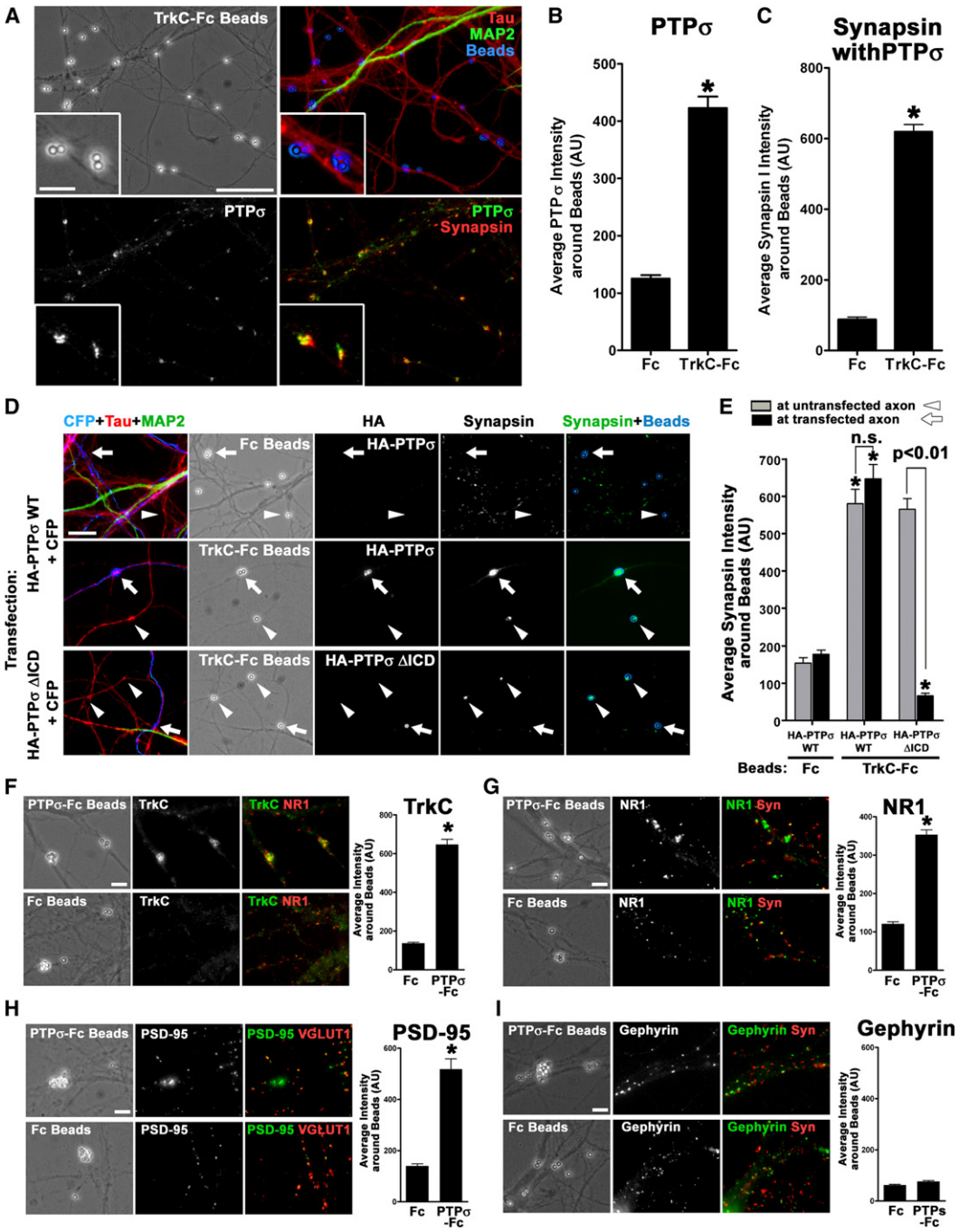

Figure 4. TrkC and PTPσ Ectodomains Induce Excitatory Presynaptic and Postsynaptic Differentiation, Respectively

(A) TrkC-Fc attached to inert beads induces local clustering of endogenous PTPσ and synapsin at axon-contact sites in hippocampal cultures. Scale bars: 20 μm; 5 μm in inset.

(B and C) Quantification of average intensity of PTPσ (B) and synapsin (C) around beads coated with TrkC-Fc or Fc. *$p < 0.0001$, t test, $n > 190$ beads.

(D and E) Neurons were transfected to coexpress HA-PTPσ wild-type (WT) or intracellular domain deletion (ΔICD) along with CFP. TrkC-Fc induced clustering of synapsin at axon-bead-contact sites equally in nontransfected (arrowheads) and transfected (arrows) axons expressing wild-type HA-PTPσ. However, TrkC-Fc clustering of synapsin was suppressed in axons expressing HA-PTPσΔICD (arrows), although HA-PTPσΔICD itself was clustered and synapsin was clustered at contacts with neighbor nontransfected axons (arrowheads). ANOVA, $p < 0.0001$, $n \geq 75$ beads each; *$p < 0.01$ compared with Fc by Dunnett's multiple comparison test. Scale bar: 20 μm.

(F–I) PTPσ-Fc, but not Fc control, attached to inert beads induces local clustering of endogenous TrkC (F), NR1 (G), and PSD-95 (H) but not of gephyrin (I) at dendrite contact sites. *$p < 0.0001$, t test, $n \geq 43$ beads each; for gephyrin, $p = 0.012$, t test. Scale bars: 10 μm. All error bars are SEM. See also Figure S4.

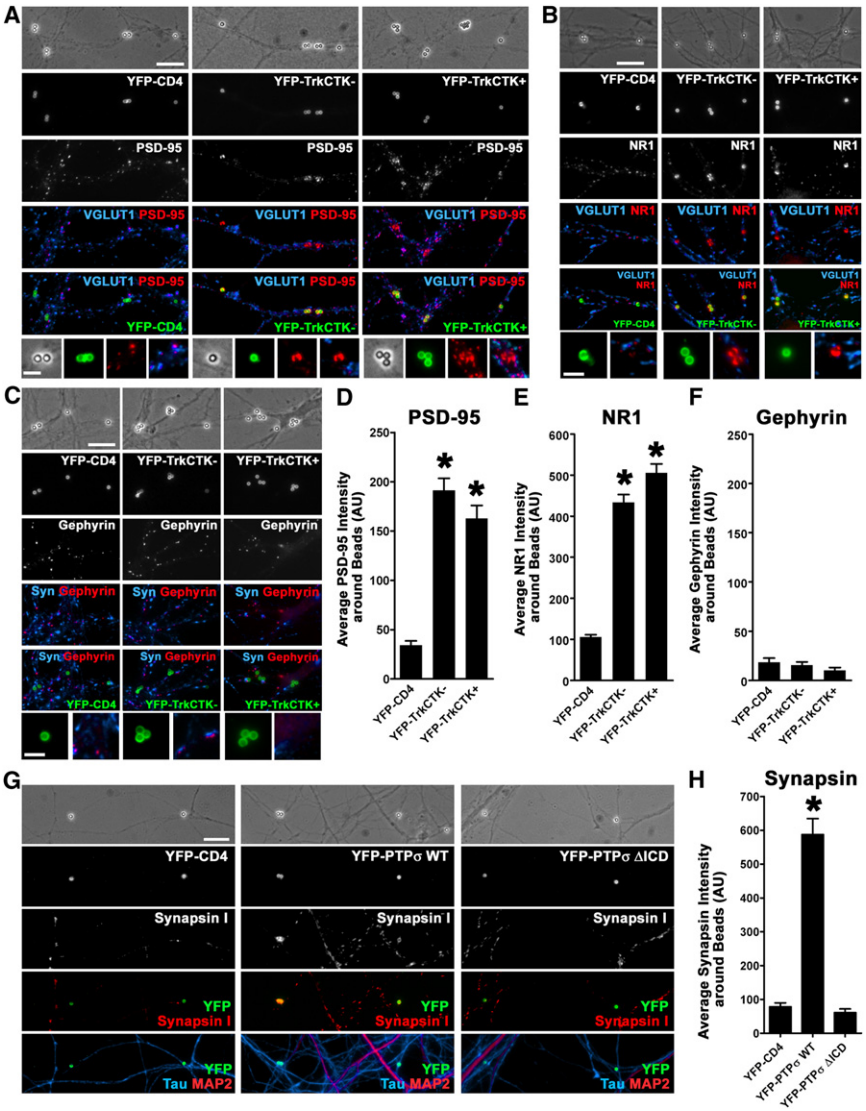

Figure 5. Aggregation of TrkC or PTPσ on the Neuron Surface Mediates Postsynaptic and Presynaptic Differentiation, Respectively

(A–C) Neurons were transfected to express at low level TrkCTK-, TrkCTK+, or control CD4 tagged extracellularly with YFP. The YFP-tagged proteins were aggregated by addition of beads coated with anti-YFP antibodies. This direct surface aggregation of YFP-TrkC TK- or TK+ but not of CD4 in dendrites resulted in coclustering of PSD-95 (A) and NR1 (B) at sites lacking VGLUT1, but no clustering of gephyrin (C). Scale bars: 10 μm; 2 μm in inset.

(D–F) Quantification of the average intensity of PSD-95 (D), NR1 (E), and gephyrin (F) around beads that aggregated YFP-tagged proteins on the dendrite surface. ANOVA, $p < 0.0001$ for PSD-95 and NR1; $p > 0.1$ for gephyrin, $n > 100$ beads each; *$p < 0.01$ compared with YFP-CD4 by Dunnett's multiple comparison test.

(G) Neurons were transfected to express at low level PTPσ wild-type (WT) or intracellular deletion (ΔICD) or control CD4 tagged extracellularly with YFP. The YFP-tagged proteins were aggregated by addition of beads coated with anti-YFP antibodies. This direct surface aggregation of YFP-PTPσ but not of CD4 in axons resulted in coclustering of synapsin, an activity requiring the intracellular domain of PTPσ. Unlike endogenous synapses, these PTPσ–mediated synapsin clusters occurred at bead contacts in isolated tau-positive axons lacking MAP2-positive dendrite contact. Scale bar: 10 μm.

(H) Quantification of the average intensity of synapsin around beads that aggregated YFP-tagged proteins on the axon surface. ANOVA, $p < 0.0001$, $n > 45$ beads each; *$p < 0.01$ compared with YFP-CD4 by Dunnett's multiple comparison test. All error bars are SEM.

induced clustering of endogenous dendritic TrkC with NMDA receptor subunit NR1 (Figure 4F). NR1 clusters induced by PTPσ-Fc-coated beads were not apposed to synapsin (Figure 4G), indicating that these NR1 clusters were not associated with interneuronal synapses. PTPσ-Fc-coated beads also induced clustering of PSD-95 but not of gephyrin (Figures 4H and 4I). We also confirmed in the coculture assay that COS cells expressing PTPσ-CFP induced clustering of NR1 (data not shown) and of PSD-95 but not of gephyrin (Figure S4G) on contacting dendrites. These data indicate that PTPσ acts as a presynaptic factor to induce excitatory postsynaptic differentiation and suggest that its postsynaptic receptor is TrkC.

Surface Aggregation of TrkC or PTPσ Mediates Postsynaptic or Presynaptic Differentiation, Respectively

Next, we tested whether PTPσ-induced clustering of TrkC on dendrites is a primary signal for triggering coclustering of excitatory postsynaptic receptors and scaffold proteins or a mere secondary and passive phenomenon. To address this, we locally aggregated surface YFP-TrkC on dendrites of transfected hippocampal neurons by using beads coated with anti-YFP antibodies. Bead-induced aggregation of YFP-TrkCTK- or YFP-TrkCTK+ on the dendrite surface resulted in significant coclustering of PSD-95 and NR1 but not of gephyrin (Figures 5A–5F). Aggregation of YFP-CD4 negative control had no significant effects on clustering of either excitatory or inhibitory postsynaptic proteins. These results indicate that surface aggregation of TrkC on dendrites is sufficient to mediate glutamatergic postsynaptic differentiation.

We also tested whether TrkC-induced aggregation of PTPσ on axons is a primary signal for triggering coclustering of presynaptic components. In axons of hippocampal neurons transfected with YFP-PTPσ, bead-induced aggregation of YFP-PTPσ, but not of YFP-PTPσΔICD, resulted in significant coclustering of synapsin (Figures 5G and 5H). Thus, PTPσ mediates presynaptic differentiation via its intracellular region.

Antibody Blockade of the TrkC-PTPσ Interaction Inhibits Synaptogenic Activities of TrkC and PTPσ and Reduces Excitatory Synapse Number

To obtain direct evidence about the involvement of the TrkC-PTPσ interaction in excitatory synapse development, we explored the ability of TrkC antibodies to neutralize this interaction. The rabbit monoclonal antibody C44H5 against TrkC recognizes a part of the LRRCC region (data not shown) within the synaptogenic PTPσ-binding domain of TrkC (Figures 1 and 2). Thus, first we tested whether TrkC antibody C44H5 blocks TrkC-PTPσ interaction. We mixed soluble TrkC-Fc with C44H5, or rabbit polyclonal anti-TrkA antibody as a negative control, in a range of concentrations and then applied the mixture to PTPσ-expressing COS cells. C44H5 blocks the binding of TrkC-Fc to PTPσ in a dose-dependent manner (Figure 6A) with a half-maximum neutralizing dose (ND50) of about 2.2 μg/ml.

Next, we tested whether C44H5 blocks synaptogenic activity of TrkC. We applied ~10 μg/ml C44H5 or nonimmunized rabbit control IgG to cocultures of hippocampal neurons with COS cells expressing TrkCTK- or control neuroligin-2. TrkC antibody C44H5 almost completely blocked synapsin clustering induced by TrkCTK- but had no effect on synapsin clustering induced by neuroligin-2 (Figures 6B and 6C). We also tested whether C44H5 blocks synaptogenic activity of PTPσ. We applied ~10 μg/ml C44H5 or control IgG to hippocampal neurons treated with PTPσ-Fc-coated beads or neurexin1β-Fc-coated control beads. C44H5 significantly yet partially suppressed PSD-95 clustering induced by PTPσ-Fc beads but had no effect on PSD-95 clustering induced by neurexin1β-Fc beads (Figures 6D and 6E). Thus, C44H5 is a neutralizing antibody that inhibits bidirectional synaptogenic activity of the TrkC-PTPσ complex.

Finally, we tested by using C44H5 whether the endogenous TrkC-PTPσ interaction is essential for synapse formation in cultured hippocampal neurons. We treated cultured hippocampal neurons with ~10 μg/ml of C44H5 or control IgG every day from DIV 9 to DIV 12, and then analyzed synapse markers at DIV12.5. The chronic treatment with C44H5 significantly reduced the densities of clusters of VGLUT1 (Figures 6F and 6G), PSD-95 (Figure 6F; quantitative data not shown), and VGLUT1-positive PSD-95 (Figures 6F and 6H). C44H5 had no significant effects on either VGAT or VGAT-positive gephyrin cluster density (Figures 6I–6K). These data indicate that interaction between endogenous TrkC and PTPσ controls excitatory but not inhibitory synapse formation.

Knockdown of TrkC Reduces Excitatory Synapse Number in Culture and in Vivo, an Effect Rescued by Noncatalytic TrkC

Next, we tested whether endogenous TrkC is required for synapse formation in hippocampal or cortical neurons by RNA interference. We generated two independent short-hairpin RNA (shRNA) constructs for knockdown of all isoforms of TrkC (sh-TrkC#1, sh-TrkC#2). Both sh-TrkC#1 and sh-TrkC#2 reduced expression of recombinant TrkCTK- and TrkCTK+ to <15% in HEK cells and reduced endogenous TrkC immunofluorescence on hippocampal dendrites to ~35% compared to shRNA vector-transfected control (Figures S5A–S5D).

Knockdown of endogenous TrkC in cultured hippocampal neurons by either sh-TrkC#1 or shTrkC#2 reduced excitatory synapse density assessed by VGLUT1, PSD-95, and VGLUT1-positive PSD-95 clusters compared with control neurons transfected with empty shRNA vector (sh-vec) or control shRNA (sh-con) (Figures 7A and 7C–7E). In addition, knockdown of TrkC caused a significant decrease in the frequency, but not the amplitude, of AMPA-mediated miniature excitatory postsynaptic currents (mEPSCs) compared to control neurons transfected with sh-con, consistent with the reduced excitatory synapse density (Figures 7G–7I). Knockdown of TrkC by the two shRNA vectors had no significant effect on densities of inhibitory synaptic markers VGAT, gephyrin, or VGAT-positive gephyrin clusters (Figures 7B and 7F). The reduction of VGLUT1, PSD-95, and VGLUT1-positive PSD-95 cluster densities by sh-TrkC was fully rescued by expression of TrkCTK-* resistant to both sh-TrkC#1 and sh-TrkC#2 (Figures 7A and 7C–7E). These data indicate that endogenous TrkC is required for excitatory synapse formation through a mechanism not requiring its tyrosine kinase activity.

We further tested the effect of knockdown of TrkC in cortical layer II/III neurons in vivo by in utero electroporation at E15.5 and analysis at P32. As in neuron culture, sh-TrkC#1 reduced TrkC immunofluorescence to ~35% compared with nontransfected neighbors (Figures S6B and S6C). In pyramidal neurons in vivo, dendritic spines are a morphological marker of excitatory synapse density (Harris et al., 1992; Knott et al., 2006), more accurately assessed in sparsely transfected preparations than immunofluorescence for molecular markers considering the high-synapse density of the neuropil. The density of dendritic protrusions on secondary and tertiary dendrites in layers I and II was significantly reduced by sh-TrkC#1 compared with sh-con and was fully rescued by expression of TrkCTK-* (Figures 8A–8D). Thus, endogenous TrkC is required for spine formation in vivo through a mechanism not requiring its tyrosine kinase activity.

DISCUSSION

In this study, from an unbiased neuron-fibroblast coculture screen, we identified the neurotrophin receptor TrkC as a synaptogenic adhesion molecule responsible for excitatory synapse development. Furthermore, we identified the receptor-type tyrosine phosphatase PTPσ as the high-affinity presynaptic receptor of TrkC. All TrkC isoforms including noncatalytic forms presented to axons trigger excitatory presynaptic differentiation via trans binding to axonal PTPσ. The synaptogenic activity of TrkC requires neither its tyrosine kinase activity nor NT-3 binding but does require the PTPσ-binding LRR plus Ig1 regions of the ectodomain. Conversely, the PTPσ ectodomain presented to dendrites triggers excitatory postsynaptic differentiation associated with clustering of dendritic TrkC. Artificial aggregation of surface TrkCTK- or TrkCTK+ on dendrites alone triggers excitatory postsynaptic differentiation and aggregation of surface PTPσ on axons alone triggers presynaptic differentiation. Endogenous TrkC and PTPσ localize to excitatory synapses in hippocampal culture and in vivo. Furthermore, two independent loss-of-function experiments (antibody-based neutralization of

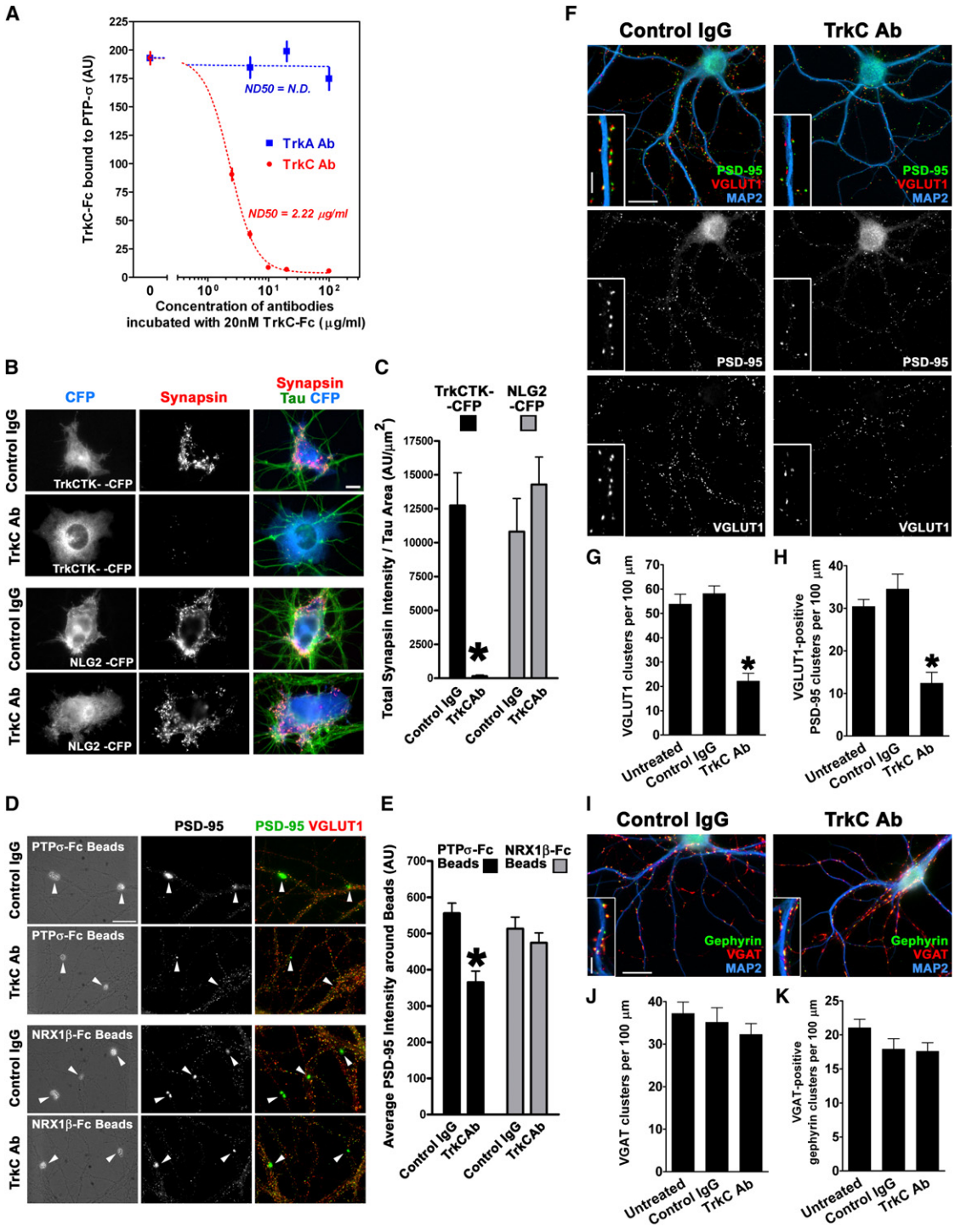

Figure 6. Blockade of TrkC-PTPσ Interaction with a Neutralizing Antibody Inhibits Synaptogenic Activity of TrkC and PTPσ and Reduces Excitatory Synapse Density

(A) A TrkC antibody against its LRRCC region (C44H5) inhibits binding of TrkC-Fc to PTPσ-CFP at half-maximum neutralizing dose (ND50) = 2.2 μg/ml (binding assay as in Figure 2). As a control, TrkA antibody had no effect.

(B and C) Addition of TrkC-neutralizing antibody compared with control nonimmune IgG at ~10 μg/ml to cocultures of COS cells expressing TrkCTK- with hippocampal neurons blocked the ability of TrkC to induce synapsin clustering. The TrkC antibody had no effect on synaptogenic activity of neuroligin-2 (NLG2). *$p < 0.0001$, t test, $n > 20$ cells each. Scale bar: 20 μm.

the TrkC-PTPσ interaction and RNAi-based knockdown of TrkC in vitro and in vivo) reveal a requirement for endogenous TrkC-PTPσ in excitatory, but not inhibitory, synapse formation. Here we propose that transsynaptic interaction between dendritic TrkC and axonal PTPσ is a specific adhesion and differentiation mechanism that bidirectionally organizes excitatory synapse development (Figure 8E).

Our findings reveal a dual function of TrkC as a glutamatergic synaptic adhesion molecule as well as a neurotrophin-3 receptor. These findings address the longstanding puzzle of why Trks have typical cell-adhesion domains (LRR and Ig) and are expressed in noncatalytic isoforms (Barbacid, 1994). Such a dual function of a neurotrophin receptor would offer a simple molecular basis for the effective local actions of diffusible trophic factors at maturing synapses. In synapse modulation induced by neurotrophins, NT-3 enhances only excitatory synapse function, whereas BDNF enhances both excitatory and inhibitory synapse function in hippocampal neurons (Vicario-Abejon et al., 2002). The excitatory-specific action of NT-3 in plasticity might be explained by this dual function of TrkC and its selective localization to glutamatergic postsynaptic sites.

Curiously, neither TrkA, TrkB, nor p75NTR exhibit any synaptogenic activity in coculture with hippocampal neurons. The relatively low homology of LRR and Ig domains among TrkA, TrkB, and TrkC (~40%–60%) may explain the TrkC-specific function. While TrkA expression is highly restricted to the peripheral nervous system and a small subset of cholinergic neurons, TrkB, like TrkC, is widely expressed in many brain regions including hippocampus and is expressed in noncatalytic forms (Barbacid, 1994). Yet TrkB ectodomain does not bind PTPσ, PTPδ, or LAR (Figure 2B). Still, it remains possible that TrkB, or even TrkA, may act as a synaptic organizing protein for a different neuron type.

Our findings also reveal a dual function of PTPσ as a glutamatergic synaptic organizing protein as well as an axon-guidance molecule (Thompson et al., 2003). We show here that PTPσ induces postsynaptic differentiation and mediates presynaptic differentiation, at least in part through binding TrkC. However, TrkC may not be the only transsynaptic binding partner of PTPσ. It was recently shown that the first two FNIII domains of PTPσ bind NGL-3 and can induce PSD-95 clustering in dendrites (Kwon et al., 2010). Furthermore, in our studies, inhibiting the interaction between TrkC and PTPσ with antibody C44H5 completely abolished the synaptogenic activity of TrkC but only partially inhibited the synaptogenic activity of PTPσ (Figures 6B–6E). Thus, PTPσ may induce postsynaptic differentiation via a cooperative action of Ig domain binding to TrkC and FNIII domain binding to NGL-3.

TrkC induces only glutamatergic presynaptic differentiation when presented to axons on COS cells, on beads, or on dendrites (Figure 1 and Figures S3 and S4). This selectivity distinguishes TrkC from NGL-3 (Woo et al., 2009) and other synaptogenic molecules including neuroligins, (Chih et al., 2005) which induce glutamatergic and GABAergic presynaptic differentiation. The greater selectivity of TrkC may relate to its high-affinity binding only to PTPσ and not to PTPδ or LAR (nor to neurexins), whereas NGL-3 binds all three type IIa PTPs with similar affinity (Kwon et al., 2010). Furthermore, PTPσ induces and TrkC mediates only glutamatergic postsynaptic differentiation (Figures 4 and 5), TrkC and PTPσ are enriched only at glutamatergic synapses in vitro and in vivo (Figure 3), and our two independent loss-of-function experiments revealed effects of the TrkC-PTPσ complex only at glutamatergic and not GABAergic synapses (Figures 6 and 7). Thus, TrkC-PTPσ is perhaps the best candidate among bidirectional excitatory synaptic organizing complexes to govern chemical matching of developing excitatory presynaptic and postsynaptic components.

Almost all known synaptogenic molecules including NGLs, neuroligins, neurexins, LRRTMs, EphBs, ephrinBs, and SynCAMs have C-terminal PDZ-domain binding sites. These PDZ-binding sequences are thought to be critical for inducing clustering of intracellular scaffolds, vesicle fusion apparatus, and postsynaptic receptors (Garner et al., 2000; Sheng and Sala, 2001). Yet TrkCTK-, TrkCTK+, and PTPσ all lack typical PDZ-binding motifs (C termini are -RHGF for TrkCTK-, -DILG for TrkCTK+, and -HYAT for PTPσ). Nevertheless, our surface protein aggregation assays (Figure 5) show that TrkCTK- and TrkCTK+ mediate clustering of PSD-95 family proteins and NR1 and that PTPσ mediates clustering of synapsin. Thus, a PDZ-binding motif at the C terminus is not essential for inducing synaptic protein clustering. Curiously, although PTPσ is structurally distinct from α-neurexins, PTPσ also functions as an α-latrotoxin receptor to stimulate neurotransmitter release (Krasnoperov et al., 2002). A likely mechanism for presynaptic recruitment requiring the intracellular region of PTPσ (Figures 4D and 4E) is binding of the second phosphatase domain (D2) to α-liprins (Pulido et al., 1995). α-Liprins directly interact with CASK, RIMs, and ERC/ELKS/CAST and are important for presynaptic differentiation in *Drosophila* and *Caenorhabditis elegans* (Stryker and Johnson, 2007). The mechanism linking TrkCTK- and TrkCTK+ to glutamatergic postsynaptic proteins is not yet known but presumably occurs via the shared extracellular, transmembrane, and 75-aa membrane-proximal intracellular region. TrkCTK- (NC2) could further recruit the scaffold protein tamalin to activate Arf6-Rac signaling (Esteban et al., 2006) and TrkCTK+ could recruit and activate PLCγ, Shc, and

(D and E) Addition of TrkC-neutralizing antibody compared to control nonimmune IgG at ~10 μg/ml to neuron cultures treated with PTPσ-Fc attached to inert beads reduced the ability of PTPσ to induce PSD-95 clustering. TrkC-neutralizing antibody had no effect on synaptogenic activity of neurexin1β (NRX1β). *$p < 0.005$, t test, $n > 50$ beads each. Scale bar: 10 μm.

(F–H) Treatment of hippocampal neurons with TrkC-neutralizing antibody at ~10 μg/ml on each of days 9, 10, 11, and 12 reduced the density of clusters of VGLUT1 (G), PSD-95 (not shown), and apposed PSD-95/VGLUT1 (H) marking excitatory synapses at day 12.5 in culture. Control nonimmune IgG had no effect. ANOVA, $p < 0.0001$, $n \geq 25$ cells each; *$p < 0.01$ compared with untreated or control IgG by Dunnett's multiple comparison test. Scale bars: 20 μm; 5um in inset.

(I–K) The same treatment with TrkC-neutralizing antibody did not alter the density of VGAT (J) or apposed gephyrin/VGAT clusters (K) marking inhibitory synapses at day 12.5 in culture (coverslips from same dishes as in panels F–H). ANOVA, $p > 0.1$, $n > 20$ cells each. Scale bars: 20 μm; 5 μm in inset. All error bars are SEM.

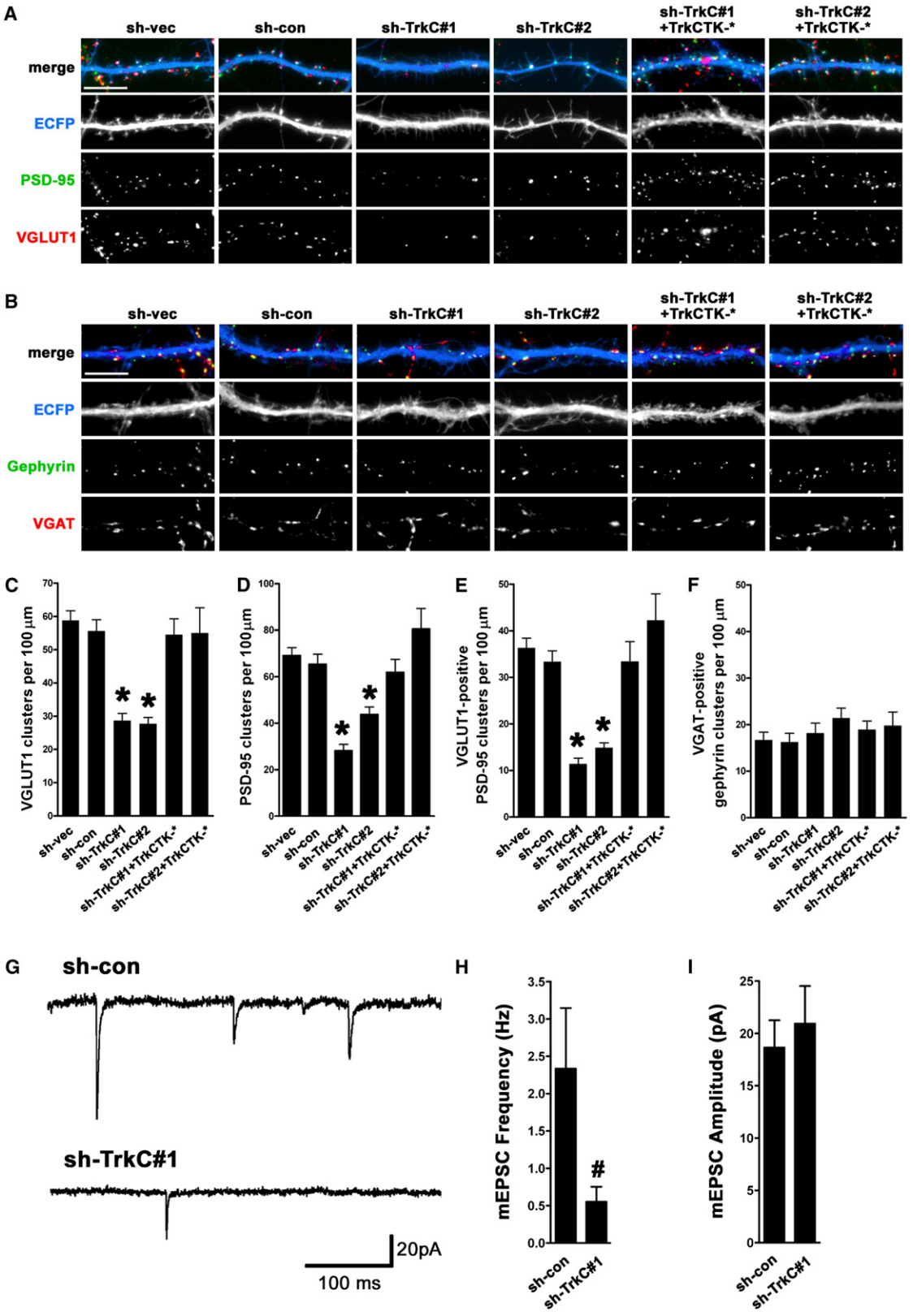
A
sh-vec
sh-con
sh-TrkC#1
sh-TrkC#2
sh-TrkC#1 +TrkCTK-*
sh-TrkC#2 +TrkCTK-*
merge
ECFP
PSD-95
VGLUT1
B
sh-vec
sh-con
sh-TrkC#1
sh-TrkC#2
sh-TrkC#1 +TrkCTK-*
sh-TrkC#2 +TrkCTK-*
merge
ECFP
Gephyrin
VGAT
C
VGLUT1 clusters per 100 μm
D
PSD-95 clusters per 100 μm
E
VGLUT1-positive PSD-95 clusters per 100 μm
F
VGAT-positive gephyrin clusters per 100 μm
sh-vec
sh-con
sh-TrkC#1
sh-TrkC#2
sh-TrkC#1+TrkCTK-*
sh-TrkC#2+TrkCTK-*
G
sh-con
sh-TrkC#1
20pA
100 ms
H
mEPSC Frequency (Hz)
#
sh-con
sh-TrkC#1
I
mEPSC Amplitude (pA)
sh-con
sh-TrkC#1

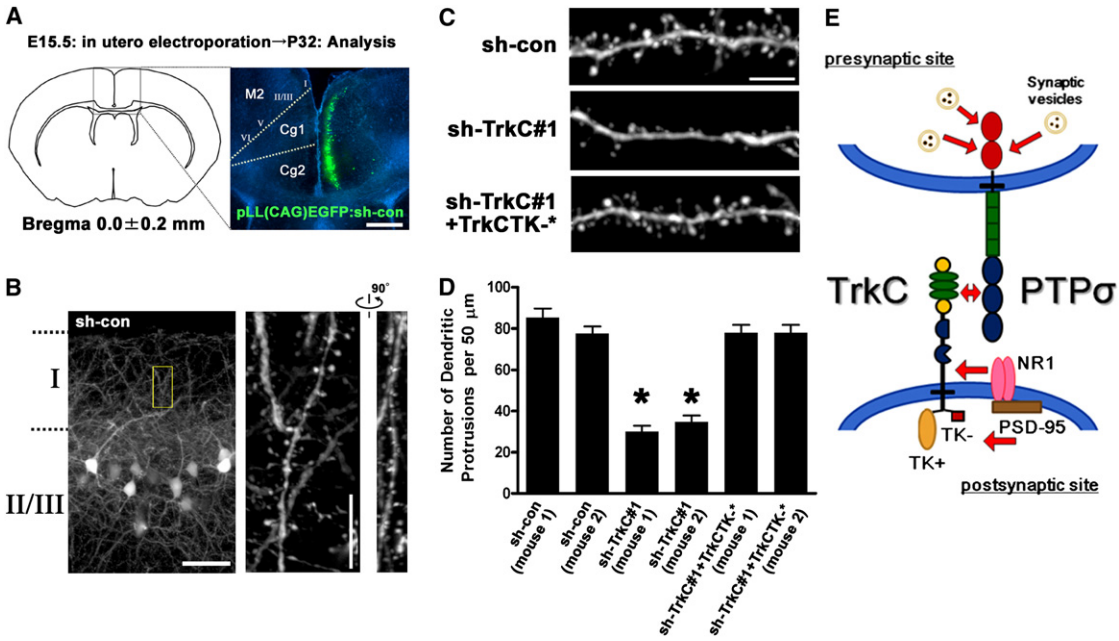

Figure 8. TrkC Knockdown Reduces Dendritic Spine Density In Vivo, an Effect Rescued by Noncatalytic TrkC

(A) In utero electroporation was performed at E15.5–E16 to transfect into neuron precursors vectors coexpressing EGFP and sh-con or sh-TrkC#1. Coronal brain slices were prepared at P32. Many GFP-positive neurons were detected in layer II/III of cingulate cortex areas 1 and 2 (Cg1 and Cg2) in each transfection condition (see also Figure S6A). For analysis, coronal sections positioned at Bregma = 0.0 ± 0.2 mm were used. Scale bar: 0.5 mm.

(B) Confocal images showing layer II/III neurons transfected with sh-con. Dendritic segments on layer I or the superficial part of layer II were selected for analysis. The rotated 3D-reconstructed image represents confocal Z-stack images used to count dendritic spines (right panel). Scale bars: 100 and 10 μm, left and middle panel, respectively.

(C) Dendrites of GFP-positive layer II/III neurons expressing sh-con, sh-TrkC#1, or sh-TrkC#1 plus TrkCTK-*. TrkC knockdown reduced the density of dendritic spines. Coexpression of TrkCTK-* rescued the effect of TrkC knockdown on spine density. Scale bar: 5 μm.

(D) Quantification of dendritic protrusion density. All morphological types of dendritic spines were counted, including filopodia-like thin protrusions which comprised only a small fraction of the total for all conditions. Each of the two animals per treatment group showed essentially the same density. ANOVA, $p < 0.0001$, $n \geq 14$ dendritic segments; *$p < 0.01$ compared with sh-con by Dunnett's multiple comparison test. Dendritic spine protrusion density was also significantly lower in the sh-TrkC#1 group when data from multiple animals were pooled for anlysis (ANOVA, $p < 0.0001$; sh-TrkC#1, $p < 0.01$ compared with sh-con by Dunnett's multiple comparison test). All error bars are SEM.

(E) Graphical summary depicting excitatory synaptogenesis by transsynaptic interaction between dendritic TrkC and axonal PTPσ. See also Figure S6.

Frs2 leading to Ras and PI3-kinase (Huang and Reichardt, 2003). The existence of eight alternatively spliced TrkC variants possessing different intracellular regions and a common extracellular region may contribute to diversity of glutamatergic postsynaptic composition.

We show here that TrkC is required in cortical neurons in vivo for development of dendritic spines, a function that does not require TrkC kinase activity (Figures 8A–8D). These data indicate a noncatalytic function of TrkC in morphological excitatory synaptogenesis in vivo. Linkage of *NTRK3* to panic disorder (Armengol et al., 2002), obsessive-compulsive disorder (Alonso et al., 2008), and childhood-onset mood disorders (Feng et al., 2008) in patients supports the importance of TrkC for cognitive function. Deletion of all TrkC isoforms in mice ($NTRK3^{-/-}$) results in earlier postnatal lethality by several weeks compared with deletion of only the kinase-active isoforms ($NTRK3^{TK-/-}$) (Klein et al., 1994; Tessarollo et al., 1997). The earlier lethality with additional loss of the noncatalytic isoforms may be in part because of

Figure 7. TrkC Knockdown Reduces Excitatory Synapse Density in Culture, an Effect Rescued by Noncatalytic TrkC

(A and B) Cultured hippocampal neurons were transfected at 9–10 DIV with a vector coexpressing ECFP and short-hairpin RNA (shRNA) constructs bearing no insert (sh-vec), control shRNA (sh-con), or two independent shRNA sequences effective to knock down TrkC (sh-TrkC#1 and sh-TrkC#2) (see Figure S5). Neurons were analyzed at 14–15 DIV. TrkC knockdown selectively reduced the density of clusters of VGLUT1, PSD-95, and VGLUT1-positive PSD-95 clusters marking excitatory synapses (A) but had no effect on VGAT or gephyrin-inhibitory synaptic markers (B). Coexpression of RNAi-resistant noncatalytic TrkC (TrkCTK-*) completely rescued the effects of TrkC knockdown on excitatory synapse density. Scale bars: 10 μm.

(C–F) Quantification of cluster densities of VGLUT1 (C), PSD-95 (D), VGLUT1-positive PSD-95 (E), and VGAT-positive gephyrin (F). ANOVA, $p < 0.0001$ for VGLUT1, PSD-95, and VGLUT1-positive PSD-95; $p > 0.1$ for VGAT-positive gephyrin, $n > 20$ cells each except sh-TrkC#2 + TrkCTK-*, $n = 12$; *$p < 0.01$ compared with sh-vec or sh-con by Dunnett's multiple comparison test.

(G–I) TrkC knockdown in cultured neurons (12–14 DIV) reduces the frequency (H) but not the amplitude (I) of AMPA-mediated mEPSCs (#$p < 0.05$, t test, $n = 8$, $n = 10$ cells, for sh-con and sh-TrkC#1, respectively). All error bars are SEM. See also Figure S5.

a defect in synaptogenesis. Brain-specific transgenic overexpression of TrkC increases anxiety-related behaviors and markedly increases hippocampal CA1 field EPSPs in vivo after classical conditioning or LTP induction (Dierssen et al., 2006; Sahun et al., 2007). Such outcomes are consistent with enhanced glutamatergic synapse development, at the expense of inhibitory GABAergic synapses, upon TrkC overexpression. However, these global genetic manipulations clearly have multiple consequences. The in vivo knockdown of TrkC performed here also did not specifically assess the role of TrkC interaction with PTPσ. A more specific TrkC knockin will be needed to precisely define the role of its interaction with PTPσ in vivo without altering NT-3 and kinase-mediated functions. Consistent with the proposed dual function of PTPσ, *Ptprs*$^{-/-}$ mice also show multiple defects, including increased lethality, ataxia, and neuroendocrine dysplasia, as well as altered hippocampal and cortical development (Elchebly et al., 1999; Meathrel et al., 2002; Wallace et al., 1999). Given the broad expression patterns of TrkC and PTPσ during development, some loss-of-function defects may be because of loss of critical trans interaction of TrkC and PTPσ outside synapses.

Our study raises a number of questions for future research. We show here that the bidirectional synaptic organizing function of TrkC-PTPσ occurs independently of kinase and phosphatase activity, but whether this interaction triggers or otherwise regulates catalytic activity is unknown. This is the first trans interaction of which we are aware between a tyrosine kinase and a tyrosine phosphatase, and it may represent a mechanism for regulating the balance of tyrosine phosphorylation. It will be important to determine whether binding of PTPσ activates TrkC kinase and/or whether binding of TrkC activates PTPσ phosphatase. It will be particularly interesting to determine how the TrkC-PTPσ adhesion complex regulates glutamatergic synaptic signaling pathways and how NT-3 modulates this process. TrkC kinase activation initiates multiple pathways including Ras-Erk1/2, Src, and PI3K-Akt (Huang and Reichardt, 2003), pathways shown to alter AMPA and NMDA-mediated transmission (Sheng and Kim, 2002). N-cadherin is a major substrate of PTPσ (Siu et al., 2007), raising the potential for TrkC-PTPσ modulation of other synaptic adhesion complexes. The distinct binding sites could allow for simultaneous binding of PTPσ and NT-3 to TrkC, via LRR-Ig1 and Ig2, respectively. NT-3 may modulate the synaptogenic activity of TrkC, for example, by inducing TrkC dimerization and internalization. PTPσ also binds via its first Ig domain to chondroitin and heparan sulfate proteoglycans to inhibit axon regeneration (Aricescu et al., 2002; Shen et al., 2009). Whether TrkC and proteoglycans compete for binding to PTPσ and consequences for axon regeneration and synaptogenic activity remain to be determined. The TrkC-PTPσ interaction may function in diverse processes including cell proliferation and differentiation, axon guidance and regeneration, and excitatory synaptic assembly and signaling.

EXPERIMENTAL PROCEDURES

Cell Cultures, Transfection, and Immunocytochemistry

Cultures of hippocampal neurons, neuron-fibroblast cocultures, and immunocytochemistry were performed essentially as described (Linhoff et al., 2009). Transfections into COS-7 cells and hippocampal neurons were done by using FuGENE 6 (Roche) and the ProFection Mammalian Transfection System (Promega), respectively. The cDNAs for full-length rat TrkCTK- (BC078844), TrkCTK+ (NM_019248), TrkCKI25 (AAB26724.1), TrkA (NM_021589), TrkBTK- (NM_001163168), TrkBTK+ (NM_012731), and p75NTR (NM_012610) were cloned by RT-PCR from a P11 rat brain cDNA library (Linhoff et al., 2009) and subcloned into pcDNA3 vectors. Deletion and swap mutants of TrkC were made based on domain structures described by Barbacid (1994). Additional details are provided in Supplemental Experimental Procedures.

Immunofluorescence in Hippocampus

For double staining with TrkC and VGLUT1 or gephyrin, adult mice were perfused intracardially with 2% paraformaldehyde in PBS. The brain was removed, postfixed for 2 hr at 4°C, cryoprotected in 30% (w/v) sucrose in PBS for 48 hr at 4°C, and frozen on dry ice. Cryostat sections (20 μm) were mounted on Superfrost Plus slides and stored at −80°C. For double staining with PTPσ and PSD-95, the brains were immediately extracted and snap-frozen in Tissue-Tek OCT compound by using isopentane cooled in dry ice and ethanol. Transverse cryostat sections were cut at 12 μm and fixed in 100% methanol for 10 min at −20°C. Sections were incubated in blocking solution (PBS + 3% bovine serum albumin [BSA] and 5% normal goat serum) with 0.25% Triton X-100 and then incubated overnight at 4°C with anti-TrkC (1:500; C44H5; Cell Signaling) and anti-VGLUT1 (1:1000; NeuroMab N28/9) or anti-gephyrin (1:1000; mAb7a; Synaptic Systems), or anti-PTPσ (IgG1; 1:500; clone 17G7.2; MediMabs) and anti-PSD-95 family (IgG2a; 1:500; clone 6G6-1C9; Thermo Scientific). DAPI (100 ng/ml) was included with appropriate secondary antibodies. Confocal images were captured sequentially at an optical thickness of 0.37 μm on a Fluoview FV500 using a 60 × 1.35 numerical aperture (NA) objective with 405, 488, and 568 nm lasers and custom filter sets.

Binding Assays

For testing binding of soluble Fc-fusion proteins, COS-7 cells on coverslips were transfected with the expression vectors and grown for 24 hr. The transfected COS cells were washed with extracellular solution (ECS) containing 168 mM NaCl, 2.4 mM KCl, 20 mM HEPES (pH 7.4), 10 mM D-glucose, 2 mM $CaCl_2$, and 1.3 mM $MgCl_2$ with 100 μg/ml BSA (ECS/BSA) and then incubated with ECS/BSA containing 100 nM purified Fc-fusion protein for 1 hr at room temperature. The cells were washed in ECS, fixed with 4% paraformaldehyde, and incubated with blocking solution and then biotin-conjugated antibodies to human IgG Fc or human IgG (H^+L) (donkey IgG; 1:1000; Jackson ImmunoResearch) and Alexa568-conjugated streptavidin (Invitrogen).

Bead Clustering Experiments

Nonfluorescent NeutrAvidin-labeled FluoSpheres (Invitrogen; F-8777; aqueous suspensions containing 1% solids) with a diameter of 1 μm were rinsed in PBS containing 100 μg/ml BSA (PBS/BSA) and incubated with either biotin-conjugated anti-GFP (here called anti-YFP; Rockland Immunochemicals) or biotin-conjugated anti-human IgG Fc (Jackson ImmunoResearch) at ~6 μg antibody per μl beads in PBS/BSA at RT for 2 hr and then rinsed in PBS/BSA. The anti-human IgG Fc-bound beads were further incubated in each soluble Fc protein at 1–2 μg Fc protein per μl beads in PBS/BSA at RT for 2 hr then rinsed in PBS/BSA. Beads were sprinkled onto hippocampal neuron cultures (1 μl per coverslip), and 1 day later the cells were fixed and stained.

In Utero Electroporation

In utero electroporation was performed as described (Tabata and Nakajima, 2001). In brief, timed pregnant CD-1 mice at 15.5–16.0 days of gestation (E15.5–E16) were anesthetized, the uterine horns were exposed, and ~1 μl DNA solution (1.5 μg/μl) mixed with Fast Green was injected into the lateral ventricle. Electroporation was performed (40 V for 50 ms, with 950 ms intervals; five pulses) with a tweezers-type electrode, which had disc electrodes of 5 mm in diameter at the tip (CUY650-5; Tokiwa Science). Embryos were then placed back into the abdominal cavity and the abdominal wall was sutured. At postnatal 32 days, mice were perfused with PBS followed by 4% paraformaldehyde in PBS. After 2 days of immersion fixation, brains were cryoprotected in 30% sucrose in 0.1 M phosphate buffer

and cut in cold PBS at 100 μm in the coronal plane with a vibratome. Brain sections were mounted on a glass slide and coverslipped with Immu-Mount (Thermo Scientific). Protocols were approved by the Animal Care Committee, consistent with Canadian Council on Animal Care and Use guidelines.

Electrophysiology

Whole-cell voltage-clamp recordings were made from cultured hippocampal pyramidal neurons (DIV12–14) that had been transfected with sh-con or sh-TrkC#1. The experimenter was blind to the DNA each neuron had received. Cells were patched under visual guidance in extracellular solution containing 140 mM NaCl, 5.4 mM KCl, 10 mM HEPES, 33 mM glucose, 1.3 mM $CaCl_2$, 1.3 mM $MgCl_2$, 0.0005 mM TTX, 0.01 mM bicuculine, and 0.05 mM D-AP5. The intracellular solution contained 130 mM $CsMeSO_4$, 10 mM HEPES, 4 mM Mg.ATP, 0.3 mM Na.GTP, 0.5 mM EGTA, 5 mM QX315.Br, and 8 mM NaCl (pH 7.2, 280 mOsm). Cells were held at −70mV and series resistance was less than 30 MΩ. Currents were recorded with the WinLTP software (Anderson and Collingridge, 2007) and analyzed offline with the Mini Analysis software (Synaptosoft).

Imaging, Quantitative Fluorescence, Spine Analysis, and Statistical Analysis

All image acquisitions, analyses, and quantifications were performed by investigators blind to the experimental condition.

For cocultures, fields for imaging were chosen only by the CFP and phase-contrast channels, for the presence of CFP-positive COS cells in a neurite-rich region. The synapsin or uptaken SynTag channel was thresholded and the total intensity of puncta within all regions positive for both CFP and dephospho-tau but negative for MAP2 was measured. The VGLUT1 or VGAT channel was thresholded and the total intensity of all puncta within CFP-positive regions was measured.

For binding of Fc-fusion proteins, measures indicate average intensity of bound Fc protein per COS cell area minus off-cell background with intensity normalized by average CFP intensity of COS cells expressing indicated CFP-tagged proteins.

For bead experiments, regions for analysis were chosen by the YFP and phase-contrast channels. Beads overlapping neurites positive for dephospho-tau but negative for MAP2 were judged as attached to axons. Beads overlapping MAP2-positive neurites were judged as attached to dendrites. After subtracting off-cell background, the average gray value associated with beads was measured by using a concentric ~2 μm circle. In the case of aggregated beads, a random two beads among them were measured.

For neurons transfected with shRNA vectors, CFP-expressing neurons were chosen randomly based on health and expression level. For TrkC-neutralizing antibody experiments, neurons were chosen randomly based on similar cell density and morphology. After images were thresholded, synaptic protein puncta were delineated by the perimeter of the transfected or designated neuron. Three regions of dendrites per neuron were randomly selected and the number of synaptic protein puncta per dendrite length was measured. VGLUT1-positive PSD-95 clusters indicate the number of clusters with pixel overlap between the separately thresholded VGLUT1 and PSD-95 channels (indicated similarly for VGAT-positive gephyrin clusters).

For dendritic spine imaging, a FluoView1000 confocal microscope fitted with a 60 × 1.42 NA oil-immersion lens and 488 nm argon laser was used to acquire images of apical secondary and tertiary dendrites of EGFP-expressing layer II/III cortical neurons in cingulate cortex area at Bregma = 0.0 ± 0.2 mm. The images were acquired at 12 bit greyscale with a pixel size of 0.11 μm, typically spanning a 70 × 70 μm area. Optical sections in the *z*-axis were acquired at 0.2 μm intervals covering at least 6 μm z-thickness. Stacked single sections and three-dimensional (3D)-reconstructed images were used jointly to count the number of spines. Spine density in at least 25 μm dendritic segments was measured. For each analyzed animal, at least 14 dendritic segments from what was estimated to be at least 10 different neurons were measured.

Analysis was performed by using Metamorph 6.1, Microsoft Excel, and GraphPad Prism 4. Statistical comparisons were made with Student's unpaired t test or one-way ANOVA with post hoc Dunnett's multiple comparison test, as indicated in the figure legends. All data are reported as the mean ± standard error of the mean (SEM).

SUPPLEMENTAL INFORMATION

Supplemental Information includes six figures and Supplemental Experimental Procedures and can be found with this article online at doi:10.1016/j.neuron.2010.12.024.

ACKNOWLEDGMENTS

We thank Dr. Michael Linhoff for his cDNA expression library and screening method, Dr. Daisaku Yokomaku for advice and technical assistance, and Xiling Zhou for excellent preparation of neuron cultures. We thank Dr. Robert Holt and team at the Michael Smith Genome Sciences Centre for arraying the cDNA subpool and preparing DNA in 384 well format. P. A. would like to thank Dr. Hillel Adesnik for his help in learning the in utero electroporation technique. This work was supported by National Institutes of Health MH070860, CIHR MOP-84241, Canada Research Chair and Michael Smith Foundation for Health Research salary awards to A.M.C., CIHR MOP-12675 to T.H.M., and by a Japan Society for the Promotion of Science Postdoctoral Fellowship for Research Abroad to H.T.

Accepted: October 29, 2010
Published: January 26, 2011

REFERENCES

Alonso, P., Gratacos, M., Menchon, J.M., Segalas, C., Gonzalez, J.R., Labad, J., Bayes, M., Real, E., de Cid, R., Pertusa, A., et al. (2008). Genetic susceptibility to obsessive-compulsive hoarding: The contribution of neurotrophic tyrosine kinase receptor type 3 gene. Genes Brain Behav. *7*, 778–785.

Anderson, W.W., and Collingridge, G.L. (2007). Capabilities of the WinLTP data acquisition program extending beyond basic LTP experimental functions. J. Neurosci. Methods *162*, 346–356.

Aricescu, A.R., McKinnell, I.W., Halfter, W., and Stoker, A.W. (2002). Heparan sulfate proteoglycans are ligands for receptor protein tyrosine phosphatase sigma. Mol. Cell. Biol. *22*, 1881–1892.

Armengol, L., Gratacos, M., Pujana, M.A., Ribases, M., Martin-Santos, R., and Estivill, X. (2002). 5′ UTR-region SNP in the NTRK3 gene is associated with panic disorder. Mol. Psychiatry *7*, 928–930.

Barbacid, M. (1994). The Trk family of neurotrophin receptors. J. Neurobiol. *25*, 1386–1403.

Chih, B., Engelman, H., and Scheiffele, P. (2005). Control of excitatory and inhibitory synapse formation by neuroligins. Science *307*, 1324–1328.

Chubykin, A.A., Atasoy, D., Etherton, M.R., Brose, N., Kavalali, E.T., Gibson, J.R., and Sudhof, T.C. (2007). Activity-dependent validation of excitatory versus inhibitory synapses by neuroligin-1 versus neuroligin-2. Neuron *54*, 919–931.

Dalva, M.B., McClelland, A.C., and Kayser, M.S. (2007). Cell adhesion molecules: Signalling functions at the synapse. Nat. Rev. Neurosci. *8*, 206–220.

de Wit, J., Sylwestrak, E., O'Sullivan, M.L., Otto, S., Tiglio, K., Savas, J.N., Yates, J.R., 3rd, Comoletti, D., Taylor, P., and Ghosh, A. (2009). LRRTM2 interacts with Neurexin1 and regulates excitatory synapse formation. Neuron *64*, 799–806.

Dierssen, M., Gratacos, M., Sahun, I., Martin, M., Gallego, X., Amador-Arjona, A., Martinez de Lagran, M., Murtra, P., Marti, E., Pujana, M.A., et al. (2006). Transgenic mice overexpressing the full-length neurotrophin receptor TrkC exhibit increased catecholaminergic neuron density in specific brain areas and increased anxiety-like behavior and panic reaction. Neurobiol. Dis. *24*, 403–418.

Elchebly, M., Wagner, J., Kennedy, T.E., Lanctot, C., Michaliszyn, E., Itie, A., Drouin, J., and Tremblay, M.L. (1999). Neuroendocrine dysplasia in mice lacking protein tyrosine phosphatase sigma. Nat. Genet. *21*, 330–333.

Esteban, P.F., Yoon, H.Y., Becker, J., Dorsey, S.G., Caprari, P., Palko, M.E., Coppola, V., Saragovi, H.U., Randazzo, P.A., and Tessarollo, L. (2006). A kinase-deficient TrkC receptor isoform activates Arf6-Rac1 signaling through the scaffold protein tamalin. J. Cell Biol. *173*, 291–299.

Feng, Y., Vetro, A., Kiss, E., Kapornai, K., Daroczi, G., Mayer, L., Tamas, Z., Baji, I., Gadoros, J., King, N., et al. (2008). Association of the neurotrophic tyrosine kinase receptor 3 (NTRK3) gene and childhood-onset mood disorders. Am. J. Psychiatry *165*, 610–616.

Francks, C., Maegawa, S., Laurén, J., Abrahams, B.S., Velayos-Baeza, A., Medland, S.E., Colella, S., Groszer, M., McAuley, E.Z., Caffrey, T.M., et al. (2007). LRRTM1 on chromosome 2p12 is a maternally suppressed gene that is associated paternally with handedness and schizophrenia. Mol. Psychiatry *12*, 1129–1139, 1057.

Garner, C.C., Nash, J., and Huganir, R.L. (2000). PDZ domains in synapse assembly and signalling. Trends Cell Biol. *10*, 274–280.

Graf, E.R., Zhang, X.Z., Jin, S.X., Linhoff, M.W., and Craig, A.M. (2004). Neurexins induce differentiation of GABA and glutamate postsynaptic specializations via neuroligins. Cell *119*, 1013–1026.

Harris, K.M., Jensen, F.E., and Tsao, B. (1992). Three-dimensional structure of dendritic spines and synapses in rat hippocampus (CA1) at postnatal day 15 and adult ages: Implications for the maturation of synaptic physiology and long-term potentiation. J. Neurosci. *12*, 2685–2705.

Huang, E.J., and Reichardt, L.F. (2003). Trk receptors: Roles in neuronal signal transduction. Annu. Rev. Biochem. *72*, 609–642.

Jamain, S., Quach, H., Betancur, C., Rastam, M., Colineaux, C., Gillberg, I.C., Soderstrom, H., Giros, B., Leboyer, M., Gillberg, C., and Bourgeron, T. (2003). Mutations of the X-linked genes encoding neuroligins NLGN3 and NLGN4 are associated with autism. Nat. Genet. *34*, 27–29.

Johnson, K.G., and Van Vactor, D. (2003). Receptor protein tyrosine phosphatases in nervous system development. Physiol. Rev. *83*, 1–24.

Kim, H.G., Kishikawa, S., Higgins, A.W., Seong, I.S., Donovan, D.J., Shen, Y., Lally, E., Weiss, L.A., Najm, J., Kutsche, K., et al. (2008). Disruption of neurexin 1 associated with autism spectrum disorder. Am. J. Hum. Genet. *82*, 199–207.

Klein, R., Silos-Santiago, I., Smeyne, R.J., Lira, S.A., Brambilla, R., Bryant, S., Zhang, L., Snider, W.D., and Barbacid, M. (1994). Disruption of the neurotrophin-3 receptor gene trkC eliminates la muscle afferents and results in abnormal movements. Nature *368*, 249–251.

Knott, G.W., Holtmaat, A., Wilbrecht, L., Welker, E., and Svoboda, K. (2006). Spine growth precedes synapse formation in the adult neocortex in vivo. Nat. Neurosci. *9*, 1117–1124.

Ko, J., Fuccillo, M.V., Malenka, R.C., and Sudhof, T.C. (2009). LRRTM2 functions as a neurexin ligand in promoting excitatory synapse formation. Neuron *64*, 791–798.

Krasnoperov, V., Bittner, M.A., Mo, W., Buryanovsky, L., Neubert, T.A., Holz, R.W., Ichtchenko, K., and Petrenko, A.G. (2002). Protein-tyrosine phosphatase-sigma is a novel member of the functional family of alpha-latrotoxin receptors. J. Biol. Chem. *277*, 35887–35895.

Kwon, S.K., Woo, J., Kim, S.Y., Kim, H., and Kim, E. (2010). Trans-synaptic adhesions between netrin-G ligand-3 (NGL-3) and receptor tyrosine phosphatases LAR, protein-tyrosine phosphatase delta (PTPdelta), and PTPsigma via specific domains regulate excitatory synapse formation. J. Biol. Chem. *285*, 13966–13978.

Linhoff, M.W., Lauren, J., Cassidy, R.M., Dobie, F.A., Takahashi, H., Nygaard, H.B., Airaksinen, M.S., Strittmatter, S.M., and Craig, A.M. (2009). An unbiased expression screen for synaptogenic proteins identifies the LRRTM protein family as synaptic organizers. Neuron *61*, 734–749.

McAllister, A.K. (2001). Neurotrophins and neuronal differentiation in the central nervous system. Cell. Mol. Life Sci. *58*, 1054–1060.

Meathrel, K., Adamek, T., Batt, J., Rotin, D., and Doering, L.C. (2002). Protein tyrosine phosphatase sigma-deficient mice show aberrant cytoarchitecture and structural abnormalities in the central nervous system. J. Neurosci. Res. *70*, 24–35.

Poo, M.M. (2001). Neurotrophins as synaptic modulators. Nat. Rev. Neurosci. *2*, 24–32.

Pulido, R., Serra-Pages, C., Tang, M., and Streuli, M. (1995). The LAR/PTP delta/PTP sigma subfamily of transmembrane protein-tyrosine-phosphatases: Multiple human LAR, PTP delta, and PTP sigma isoforms are expressed in a tissue-specific manner and associate with the LAR-interacting protein LIP.1. Proc. Natl. Acad. Sci. USA *92*, 11686–11690.

Sahun, I., Delgado-Garcia, J.M., Amador-Arjona, A., Giralt, A., Alberch, J., Dierssen, M., and Gruart, A. (2007). Dissociation between CA3-CA1 synaptic plasticity and associative learning in TgNTRK3 transgenic mice. J. Neurosci. *27*, 2253–2260.

Scheiffele, P., Fan, J.H., Choih, J., Fetter, R., and Serafini, T. (2000). Neuroligin expressed in nonneuronal cells triggers presynaptic development in contacting axons. Cell *101*, 657–669.

Segal, R.A., and Greenberg, M.E. (1996). Intracellular signaling pathways activated by neurotrophic factors. Annu. Rev. Neurosci. *19*, 463–489.

Shen, K., and Scheiffele, P. (2010). Genetics and cell biology of building specific synapse connectivity. Annu. Rev. Neurosci. *33*, 473–507.

Shen, Y., Tenney, A.P., Busch, S.A., Horn, K.P., Cuascut, F.X., Liu, K., He, Z., Silver, J., and Flanagan, J.G. (2009). PTPsigma is a receptor for chondroitin sulfate proteoglycan, an inhibitor of neural regeneration. Science *326*, 592–596.

Sheng, M., and Kim, M.J. (2002). Postsynaptic signaling and plasticity mechanisms. Science *298*, 776–780.

Sheng, M., and Sala, C. (2001). PDZ domains and the organization of supramolecular complexes. Annu. Rev. Neurosci. *24*, 1–29.

Siddiqui, T.J., and Craig, A.M. (2010). Synaptic organizing complexes. Curr. Opin. Neurobiol., in press.

Siddiqui, T.J., Pancaroglu, R., Kang, Y., Rooyakkers, A., and Craig, A.M. (2010). LRRTMs and neuroligins bind neurexins with a differential code to cooperate in glutamate synapse development. J. Neurosci. *30*, 7495–7506.

Siu, R., Fladd, C., and Rotin, D. (2007). N-cadherin is an in vivo substrate for protein tyrosine phosphatase sigma (PTPsigma) and participates in PTPsigma-mediated inhibition of axon growth. Mol. Cell. Biol. *27*, 208–219.

Stryker, E., and Johnson, K.G. (2007). LAR, liprin alpha and the regulation of active zone morphogenesis. J. Cell Sci. *120*, 3723–3728.

Sudhof, T.C. (2008). Neuroligins and neurexins link synaptic function to cognitive disease. Nature *455*, 903–911.

Tabata, H., and Nakajima, K. (2001). Efficient in utero gene transfer system to the developing mouse brain using electroporation: Visualization of neuronal migration in the developing cortex. Neuroscience *103*, 865–872.

Tessarollo, L., Tsoulfas, P., Donovan, M.J., Palko, M.E., Blair-Flynn, J., Hempstead, B.L., and Parada, L.F. (1997). Targeted deletion of all isoforms of the trkC gene suggests the use of alternate receptors by its ligand neurotrophin-3 in neuronal development and implicates trkC in normal cardiogenesis. Proc. Natl. Acad. Sci. USA *94*, 14776–14781.

Thompson, K.M., Uetani, N., Manitt, C., Elchebly, M., Tremblay, M.L., and Kennedy, T.E. (2003). Receptor protein tyrosine phosphatase sigma inhibits axonal regeneration and the rate of axon extension. Mol. Cell. Neurosci. *23*, 681–692.

Urfer, R., Tsoulfas, P., O'Connell, L., Shelton, D.L., Parada, L.F., and Presta, L.G. (1995). An immunoglobulin-like domain determines the specificity of neurotrophin receptors. EMBO J. *14*, 2795–2805.

Urfer, R., Tsoulfas, P., O'Connell, L., Hongo, J.A., Zhao, W., and Presta, L.G. (1998). High resolution mapping of the binding site of TrkA for nerve growth factor and TrkC for neurotrophin-3 on the second immunoglobulin-like domain of the Trk receptors. J. Biol. Chem. *273*, 5829–5840.

Valenzuela, D.M., Maisonpierre, P.C., Glass, D.J., Rojas, E., Nunez, L., Kong, Y., Gies, D.R., Stitt, T.N., Ip, N.Y., and Yancopoulos, G.D. (1993). Alternative forms of rat TrkC with different functional capabilities. Neuron *10*, 963–974.

Varoqueaux, F., Aramuni, G., Rawson, R.L., Mohrmann, R., Missler, M., Gottmann, K., Zhang, W., Sudhof, T.C., and Brose, N. (2006). Neuroligins determine synapse maturation and function. Neuron *51*, 741–754.

Vicario-Abejon, C., Owens, D., McKay, R., and Segal, M. (2002). Role of neurotrophins in central synapse formation and stabilization. Nat. Rev. Neurosci. *3*, 965–974.

Wallace, M.J., Batt, J., Fladd, C.A., Henderson, J.T., Skarnes, W., and Rotin, D. (1999). Neuronal defects and posterior pituitary hypoplasia in mice lacking the receptor tyrosine phosphatase PTPsigma. Nat. Genet. *21*, 334–338.

Woo, J., Kwon, S.K., Choi, S., Kim, S., Lee, J.R., Dunah, A.W., Sheng, M., and Kim, E. (2009). Trans-synaptic adhesion between NGL-3 and LAR regulates the formation of excitatory synapses. Nat. Neurosci. *12*, 428–437.